Chapter 1

Introduction

1.1 Display Technology

Display technology has been progressing promptly, since the last few years of the 21st century, especially for the flat panel display, which is an interesting area for the electronics industry, nowadays. With the popularization of computer and wireless communication, multimedia application displays and mass information interchange become important parts for people, and the demand of technologies of display mass information in contents and pictures are becoming more imperative. Furthermore, the electronic display is the main element for information display and the application of flat panel display can be widely used in many fields, such as mobile phones, camera screens, computer monitors, and televisions. Based on the various applications, the electric display includes Liquid Crystal Displays (LCDs), Plasma Display Panels (PDPs), Organic Light Emitting Diodes (OLEDs), Field Emission Displays (FEDs), and Cathode Ray Tubes (CRTs). Among all display, desired features of thin format, compact size, light weight, and high image quality can be provided by LCDs.

1.2 Liquid Crystal Displays

1.2 .1 The fundamental concept of Liquid Crystal Displays

Nowadays, LCDs have become the most attractive information displays, as the developments of the various requirements of the applications desktop monitors, mobile phones, notebooks, televisions, etc.

The first generation of Liquid Crystal Displays was dynamic scattering mode displays. However, this type of display has become more or less obsolete with the advent of twisted nematic displays, except for some special applications. The difference between these two modes is purely dielectric and non-purely dielectric effect. The dynamic scattering mode is based on the principle of dielectric as well as on conductivity alignment as the rest of LC displays including twisted nematic mode are based on purely dielectric effect.

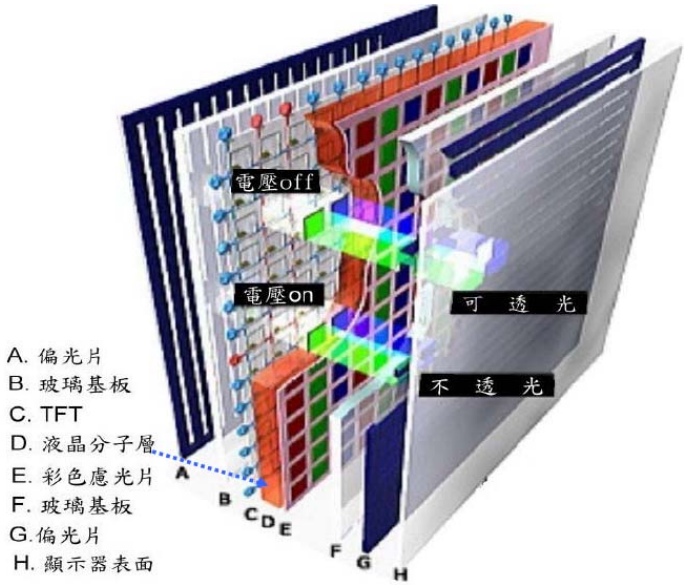

Fig. 1-1 The structure of liquid crystal display

Liquid Crystal Displays, which are passive electro-optical displays, do not generate light by itself but only modulate the light. As the development of the technology, a “transmissive type” LCD was demonstrated by Sharp Corporation in 1989 [1]. A backlight system was needed for the application of transmissive type LCD and was disposed on the rear surface. The amount of light from the backlight which transmits through the LC panel is controlled by the liquid crystal for the

purpose of displaying image. LCDs are composed of polarizer, color filter, liquid crystal, circuit plate, and backlight as shown in Fig. 1-1.

For the purpose of different kinds of applications, several types of LCDs were researched such as reflective LCD [2] and transflective LCD [3]. The transflective type is not suitable for the outdoors display, because the ambient light is stronger than the backlight. As a result, Cholesteric liquid crystal materials which can reflect specific wavelength of light were paid great attention in the research of reflective LCDs [4]. A reflector was also utilized to reflect light recently, especially the transflective LCD used an inner reflector to reflect ambient light in reflect area, while light was displayed by backlight system in transmissive area. However, several critical issues still need to be concerned, such as achievement of full-color and simplifying the fabrication process. Compared to these types of LCDs, transmissive one is still the most promising candidate for the multimedia display application. Fig. 1-2 (a) and Fig. 1-2 (b) show the three typical structures of LCDs mentioned above.

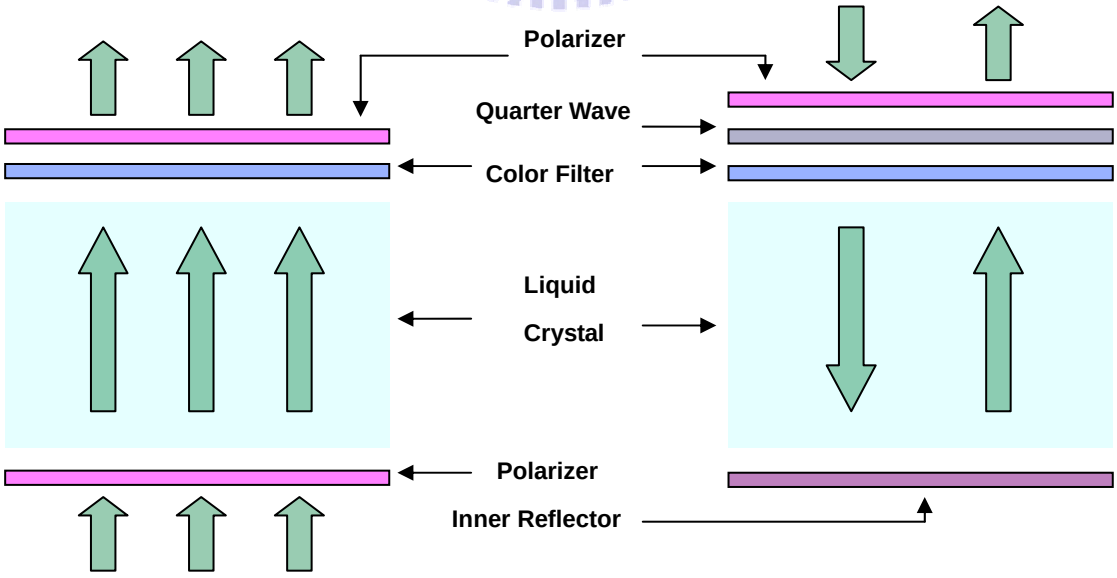

Fig. 1-2 (a) Sketch of Trnasmissive (left) and Reflective (Right) LCD

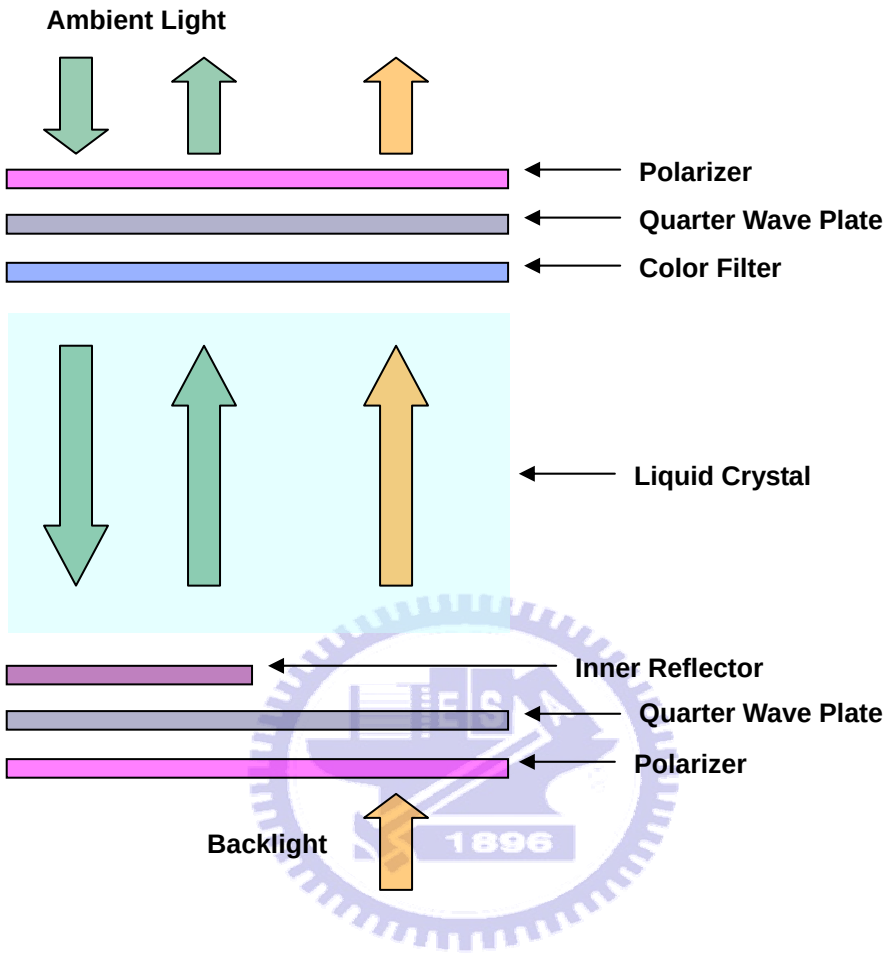

Fig. 1-2 (b) Sketch of Transflective LCD

The common LC application in transmissive LCDs is twisted nematic (TN) type. High contrast ratio and low driving voltage are its advantages; however, its slower response time is viewed as the critical drawback and restrains the application of LCDs, such as motion blur, especially for the moving picture. Based on these issues, Optical Compensation Bend (OCB) displays were investigated; because it has faster response time and wide viewing angle than those of TN type. Furthermore, adopting the plasma alignment process was the promising technique for the OCB display in this study.

1.2.2 Optically Compensated Bend (OCB) Mode

LCDs have merits such as low power consumption, slimness and lightweight and as result become widely uses as computer display. However, a conventional TN-mode LCD has a problem about viewing angle that results in degradation of the contrast ratio or inversion of the gray scale and it is not capable of displaying motion pictures optimally because of its slow response time. Furthermore, among practical display modes so far proposed, only the OCB (Optically Compensated Bend) mode can provide advantages of simultaneous fast response and wide viewing angle as well as relatively little modification needed to the conventional LCD panel manufacturing process.

Pi cell, also known as the OCB cell, was first demonstrated by P.J. Bos et al in 1984 [5]. The initial alignment of the pi cell is configured as a splay arrangement and the middle of the cell perpendicular to the substrate is aligned after applying the voltage and LC aligns to generate the bend structure. Fig. 1-3 shows the setup and basic principle of the OCB switching mode in the off (left) and on (right) state. In OCB mode, the display requires applying voltage to produce a transition from splay to bend state and the voltage is called transition voltage. However, there is a high-energy barrier, also known as Gibbs free energy, between the two states and result in the difficult transition. The free energy of the bend state with a certain voltage is lower than that of the splay state. In addition, its configuration changes to the bend state while that voltage is applied to the cell. As a result, how to shorten the transition time as much as possible to produce working bend state is a very important factor in OCB mode. In addition, this mode requires liquid crystals with high positive $\Delta\varepsilon$ values and large Δn.

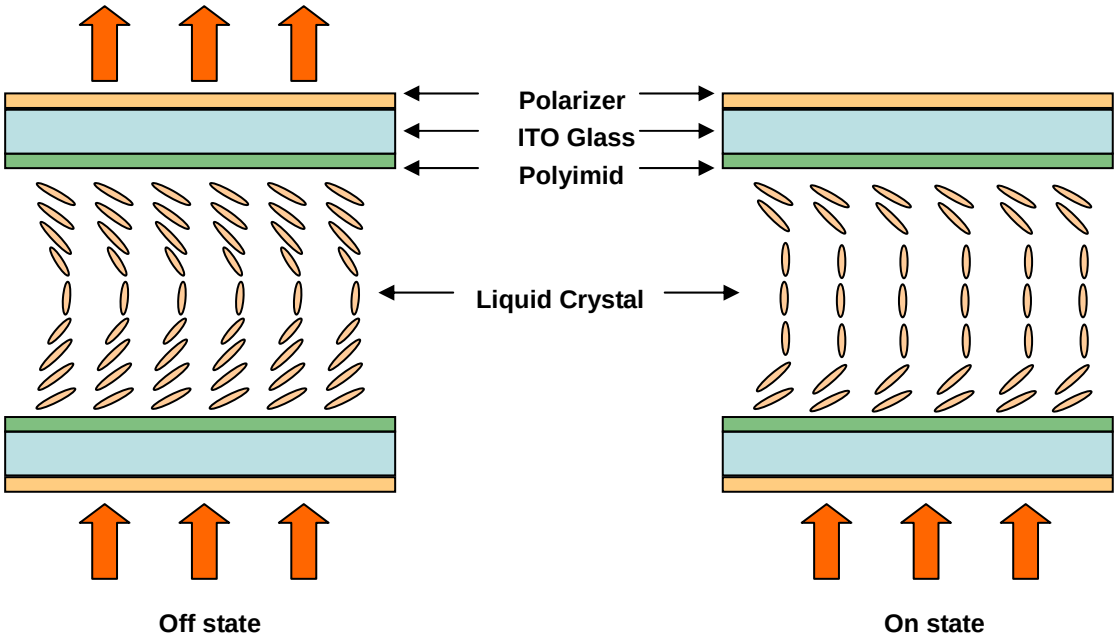

Fig. 1-3 Setup and basic principle of the OCB switching mode in the off (left) and on (right) state

As the Pi cell is used for a display application, a compensation film is required to provide the black state. The reason is that Pi cell has a biaxial birefringence in the black state attributed in its symmetrical tilt alignment near the substrate. Besides, many researches paid attention to the compensation film were investigated so far. Only one film, biaxiality is required by the film, was used to compensate for the birefringence of the black state [6]. In order to reduce the light leakage in the black state, a combination of an a-plate and c-plate was studied [7]. Furthermore, discotic films were used as the compensation films to compensate for each side of the distributed LC molecules [8 ~ 10].

Typical twisted nematic mode is well-known for the slow response to the applied electric field. However, the response of the pi cell is very rapid, and the summation of its rise and decay times is less than 10 msec, even for grey levels, for the response to the applied electric field. The reason of the rapid response of the pi cell is attributed to

be its back flow effect [11]. As shown in Fig. 1-4, the flow of the relaxation accelerates the relaxation of the center part of the cell for the case of Pi cell. Furthermore, another factor arisen from the fast response is that the area of the alignment change caused by the applied voltage is near the surface and it is highly deformed attributed to the bend configuration. As a result, field sequential display mode without color filters adopted OCB mode attributed to its rapid response time were investigated recently [12].

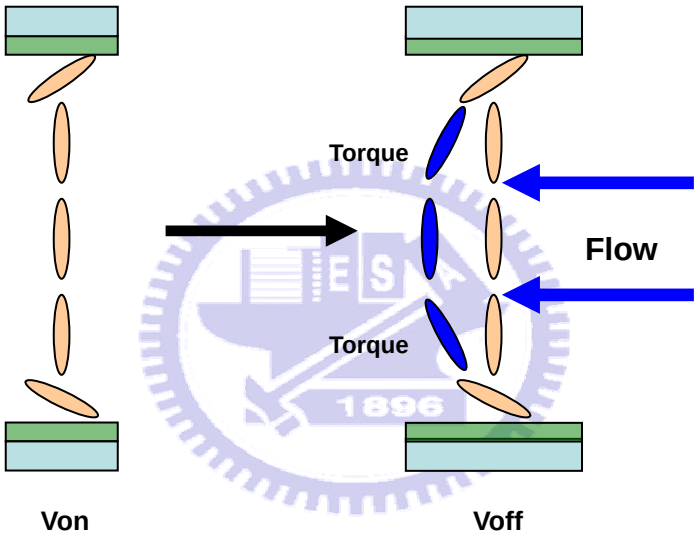

Fig. 1-4 The flow effect accelerates the relaxation motion in the center of the Pi cell

1.3 Alignment Process

Rubbing method has been adopted for alignment technologies attributed to its simple, convenient and low-cost from the early stages of LCD production in the 70s. However, while the production of TFT-LCDs started in the 80s, defects of the rubbing method were taken into lots of account. The surface of polyimide layers is rubbed with a cloth during the rubbing procedure and several problems appeared. Static

electricity, which caused by the friction between the surface of the cloth and the polyimide layers, is a critical drawback and destroys the thin film transistors (TFTs). Furthermore, Defects and stains on the surface of the alignment layer arisen from the direct contact between the surfaces and the cloth are also serious problems and restrict the development for the high definition larger sizes LCDs in the next generation.

In view of the problems mentioned above, the developments of new methods for liquid crystal alignment have been researched to take place of the conventional rubbing procedure. As a result, non-contact alignment technique had been paid into attention, such as photo-alignment and plasma beam alignment. Photo-alignment has been a focus of research since Gibbons el al. reported their photo-alignment results in 1991 [13]. In 1994, it was found that polyimide exposed to linearly polarized deep UV light showed LC alignment, and that a wider variety of materials could be used for photo-alignment [14]. At that time, viewing angle was a critical issue to be improved and multiple domain technique adopted photo-alignment technique was investigated to enhance the viewing angle attributed to its sample establishment of multiple domains. However, color shift problem cannot be addressed by multi-domain technique and that is the reason why photo-alignment did not become widespread as a mass production line. Recently, not only linearly polarized light, but also non-polarized light can be selected as the light source for the photo-alignment [15~16]. Furthermore, the relatively weak anchoring energy and non-stability by photo-alignment technique compared to the rubbing process is still a challenge to be overcome. The main progress and trends to the photo-alignment technique are summarized in Fig. 1-5. The requirements for the light sources for photo-alignment are almost the same as those for lithography except for the polarization state. In addition, high energy density light sources which can generate linearly polarized light for larger exposure area have been investigated recently.

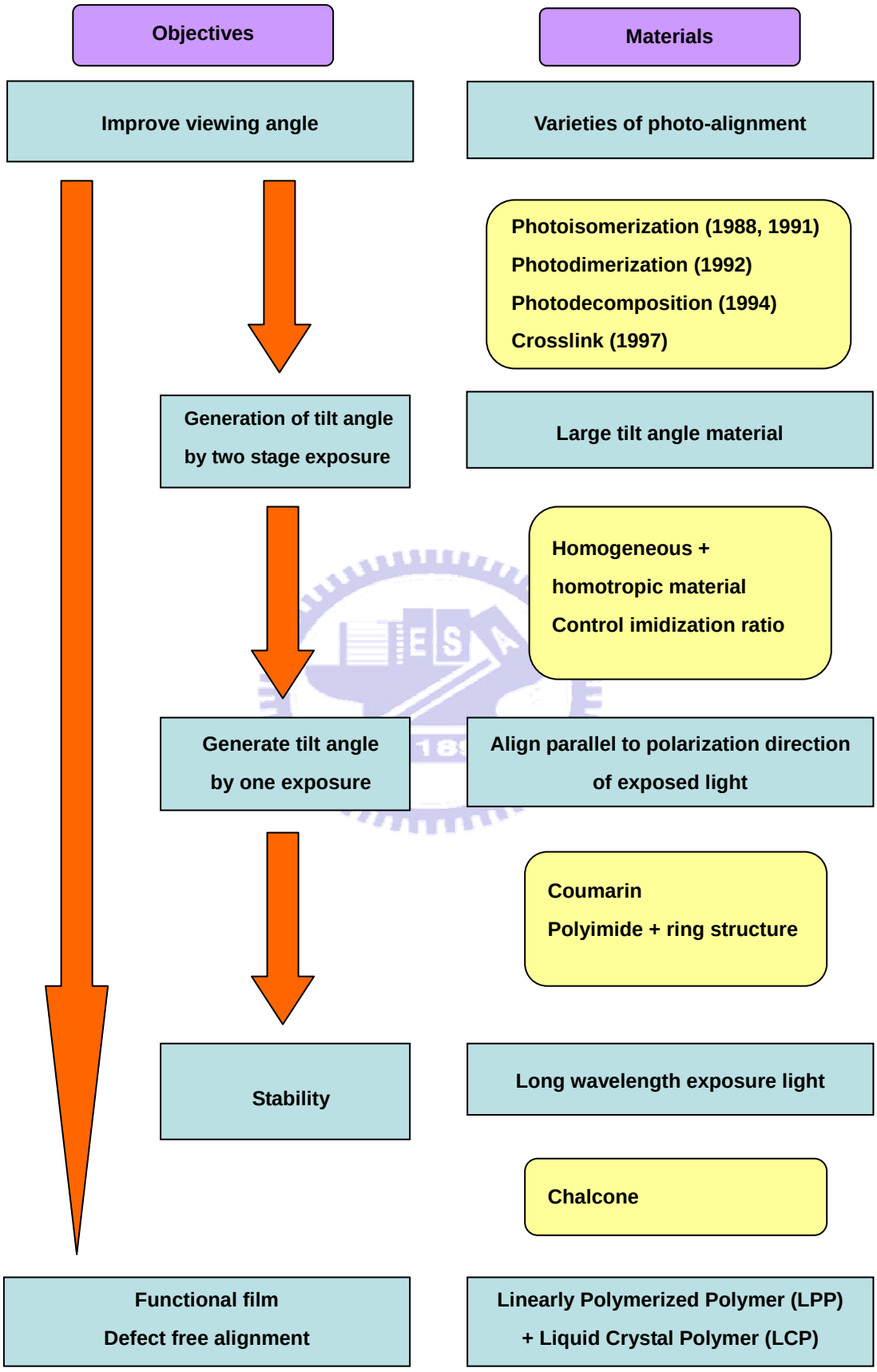

Fig. 1-5 History of the development of photo-alignment

Since photo-alignment still has some critical drawback, ALT plasma alignment technique is our solution because of its relatively higher anchoring energy and stability than that with photo-alignment. The basic construction and theory of the ALT plasma alignment technique will be described in Chapter 2 in detail.

1.4 Motivation and objective

The conventional rubbing process is used to align the alignment layer in OCB mode for a long time. However, the alignment layer is contacted directly by the roller and induces some drawbacks, such as dusts and static electricity. The drawback restricts the development of LCD production, especially for the larger size in the next generation.

As a result, ALT plasma alignment technique, which do not has the disadvantages of rubbing mentioned above, was firstly adopted for the OCB mode instead of rubbing process. Moreover, OCB has very rapid response time and is the strong candidate for the application of field sequential color display. The competitive electric-optical performance of OCB cell (response time, transmittance and surface roughness) than those of rubbing procedure was obtained and discussed in detail in the following chapters.

1.5 Organization of This Thesis

The thesis is organized as following: The fundamental principle of ALT plasma source and alignment mechanism is presented in **Chapter 2**. After that, in **Chapter 3**, the fabrication process of the OCB cells and the ALT plasma alignment procedure will be introduced in detail, and the major instruments used to investigate the electro-optic

characteristics, alignment property, pretilt angle and surface roughness of OCD cells, such as electro-optic measuring system, POM, TBA and AFM, will also be described. The experimental results and discussion, including the electro-optic performance, pretilt angle dependence, alignment property and surface morphology of OCB cells during the period of ALT plasma alignment, will be in **Chapter 4**. Finally, the conclusions of this thesis will be presented in **Chapter 5**.

Chapter 2

Principle

2.1 Introduction

Anode layer thruster (ALT) plasma system was selected as the alignment technique in this study. The fundamental concept of this technique will be described in detail in this chapter, such as history, background, theory, operation principles and the application for the LC alignment. Moreover, the alignment mechanism of this non-contact alignment technique and previous researches will also be introduced. Finally, the basic theory of the crystal rotation method will be mentioned and that is the common method to measure the pretilt angle of the LC molecules.

2.2 Discharge Characteristics

2.2.1 Plasma

Generally, the term “plasma” is used to describe a partially or completely ionized gas containing electrons, ions and neutrals. Although there is always a small degree of ionization in any gas, a stricter definition of the plasma is a “quasi-neutral gas of charged and neutral particles which exhibits collective behavior”. Quasi neutrality refers to the characteristic that positive and negative space charges balance in a given volume such that overall, the plasma is considered to be electrically neutral. The collective behavior of the plasma is result from the Coulomb forces that are long range and cause remote regions to interact with one another.

Micro-plasma show a new class of the plasma whose properties fall somewhere between those of glow discharge and arcs as shown in Fig. 2-1. These two types of processing plasma are characterized to low-pressure glow discharges and high-pressure arcs. However, the low electron temperature and non-equilibrium make them more similar to glow discharges. As a result, they are often referred to as a "high pressure glow discharges".

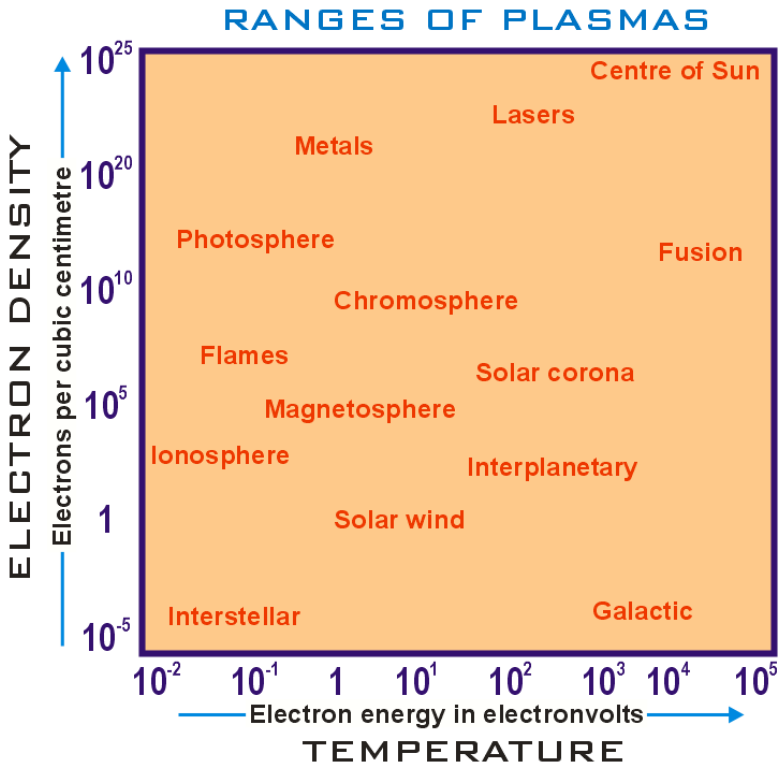

Fig. 2-1 Space and laboratory plasmas classified by their electron temperature and charged particle density

2.2.1 Glow Discharge

The name of glow discharge is the phenomenon that plasma is luminous and

depends on the geometry of the electrodes and the vessel, the gas used, the electrode material. Furthermore, the phenomenon of gas breakdown is considered as the transition from insulating state to conducting state. The associated voltage required to cause the transition is referred to as the breakdown voltage. Current flows between the electrodes via the movement of charged particles (ions and electrons) to and from the electrodes. When the electrons are energetic enough to dissociate the gas through impact to create ions, formation of a gas discharge occurs. The average electron temperature, T_e, is generally less than breakdown energy required for ionization.

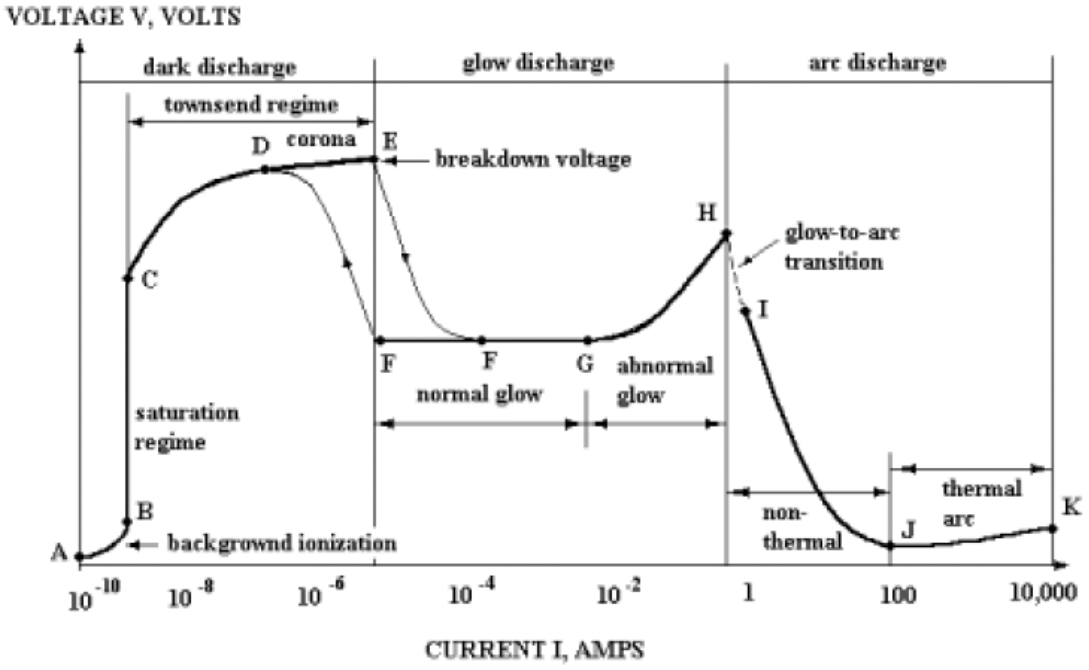

Fig. 2-2 Voltage-Current (V-I) characteristic for a discharge

When breakdown occurs, the gas suddenly becomes conductive. The current and voltage in the gas discharge vary resulting changing supply voltage. These parameters can be investigated to obtain a voltage-current (V-I) characteristic for a discharge as illustrated in Fig. 2-2. Moreover, current is limited through the discharge by using an

external ballast resistor.

Three general regions can be identified on the diagram above, the dark discharge (Townsend region), the glow discharge and the arc discharge. Because the discharge remains invisible to the eye except for corona discharge and the breakdown itself, the regime between A and E on the voltage-current characteristic is termed a dark discharge. The electric field sweeps out the ions and electrons created by ionization from background radiation during the *background ionization*. The ions and electrons migrate to the electrodes in the applied electric field producing a weak electric current. Increasing voltage results in an increasing fraction of these ions and electrons. If the voltage between the electrodes is increased far enough, eventually all the available electrons and ions are swept away, and the current saturates. The regime is named the saturation region because the current remain constant while the voltage is increased. After the voltage across the *saturation region*, the current will rise exponentially. The electric field is now high enough so the electrons initially present in the gas can acquire enough energy before reaching the anode to ionize a neutral atom. As the electric field becomes even stronger, the secondary electron may also ionize another neutral atom leading to an avalanche of electron and ion production. The regime of exponentially increasing current is called the *Townsend discharge*. The *Corona discharge* occurs in the regime of *Townsend discharge* because of high electric field near sharp points, edges, or wires in gases prior to electrical breakdown. If the coronal currents are high enough, *corona discharge* can be technically “glow discharges”, visible to the eye. For low currents, the entire corona is dark, as appropriate for the dark discharge. After the breakdown, the gas enters the *normal glow* regime, which the voltage is almost independent of the current over several orders of magnitude in the discharge current. The electrode current density is independent of the total current in this regime. This means that the plasma is in contact with only a small part of the

cathode surface at low currents. As the current is increased, the fraction of the cathode occupied by the plasma increased until plasma covers the entire cathode surface. For the next *abnormal glow* regime, the voltage increases significantly with the increasing total current in order to force the cathode current density above its natural value and provide the desired current. The third general region is arc discharge. The electrodes become sufficiently hot that the cathode emits electrons thermionically. If the DC power supply has a sufficiently low internal resistance, the discharge will undergo a glow-to-arc transition. The *arc regime*, from I through K is one where the discharge voltage decreases as the current increases, until large currents are achieved at point J, and after that the voltage increases slowly as the current increases.

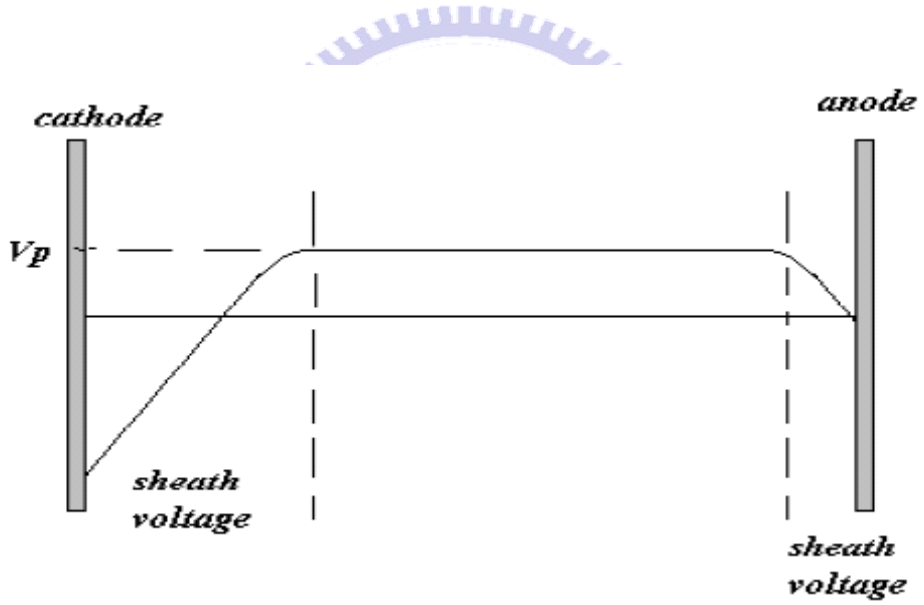

Fig. 2-3 Voltage distribution in a dc glow discharge process

Besides, the glow discharge owes its name to the fact that plasma is luminous. The glow can be produced by applying a potential difference between two electrodes in a gas. The potential drops rapidly close to the cathode, vary slowly in the plasma, and change again close to the anode. Fig. 2-3 shows the voltage distribution in a dc glow discharge process. The electric fields in the system are restricted to sheaths at

each of the electrodes. The sheath fields are such as to repel electrons trying to reach either electrode. Electrons originating at the cathode will be accelerated, collide, transfer energy, leave by diffusion and recombination, slow by the anode and get transferred into the outside circuit. The luminous glow is produced because the electrons have enough energy to generate visible light by excitation collisions. Since there is a continuous loss of electrons, there must be an equal degree of ionization going on to maintain the steady state. The energy is being continuously transferred out of the discharge and hence the energy balance must be satisfied also. Simplistically, the electrons absorb energy from the field, accelerate, ionize some atoms, and the process becomes continuous. Additional electrons are produced by secondary emission from the cathode. These are very important to maintaining a sustainable discharge.

2.3 Anode Layer Thruster (ALT) Source

2.3.1 History and Background

There has been a growing interest in recent years in ion beam surface treatment technology to meet the demands for improved surface properties of base materials for electronics and optical devices in terms of adhesion, hardness, electrical resistance and chemical stability. In order to apply the surface modification in an industrial scale, a number of requirements should be met. For example, large area irradiation, long lifetime, reliable and stable performance of the ion source. Many researches had paid attention to the ion sources with small irradiation areas. In addition, Hall thrusters, also called closed drift thrusters (CDT), have been used for the satellite propulsion in Russia during the past 30 years and was the strong candidate for the ion sources application with the large irradiation area. Two main modern variants can be classified

for the closed drift thrusters as shown in Fig. 2-4. One is anode layer thruster (ALT) and the other is stationary plasma thruster (SPT). The name “closed drift” means azimuthal drift of electrons that is general to all family of such thrusters. Stationary plasma thruster (SPT) has the extended acceleration zone compared with the anode layer thruster (ALT) and normally used for the insulator chamber walls. Notwithstanding the two have differentiating features in their operation and performance, they base on the same fundamental principles for ionizing and accelerating the propellant. These principles were first correctly optimized experimentally through the seminal work of Janes and Lowder (1965). [17]

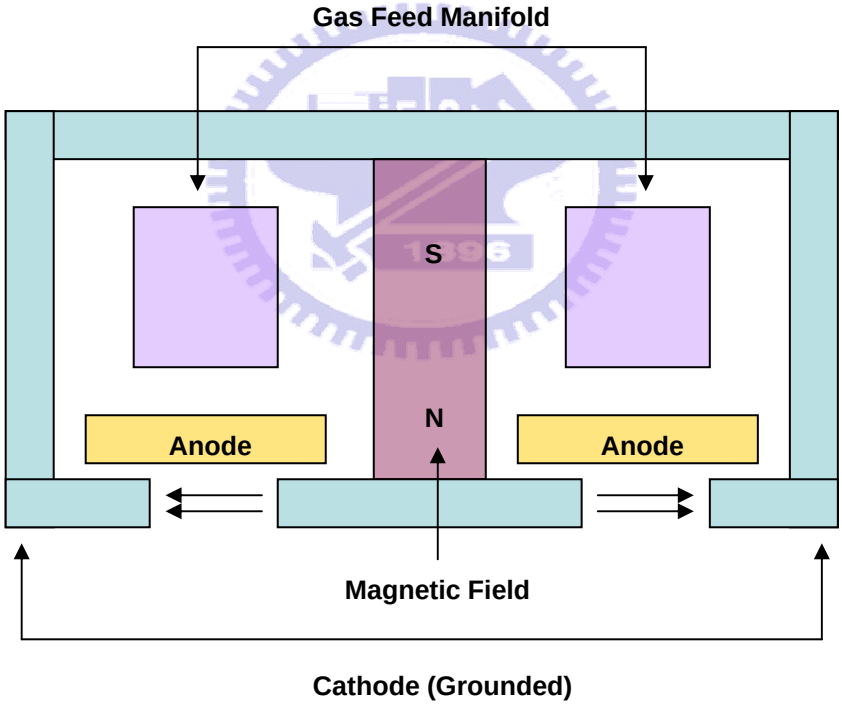

Fig. 2-4 Cross-sectional schematic drawing of the linear ion source

The plasma irradiation is generated by anode layer thruster (ALT). Fig. 2-5 shows the schematic diagram of the ALT system. The ALT source consists of outer and inner cathode and anode. Permanent magnet is necessary to generate magnet pole

at outer cathode. The plasma flux is generated by cross electric field (E) and magnetic field (H) immediately. In ALT source, several operating parameters can be selected, such as incidence, energy and exposure time. Among these parameters, exposure time is viewed as the significant factor for the plasma beam alignment.

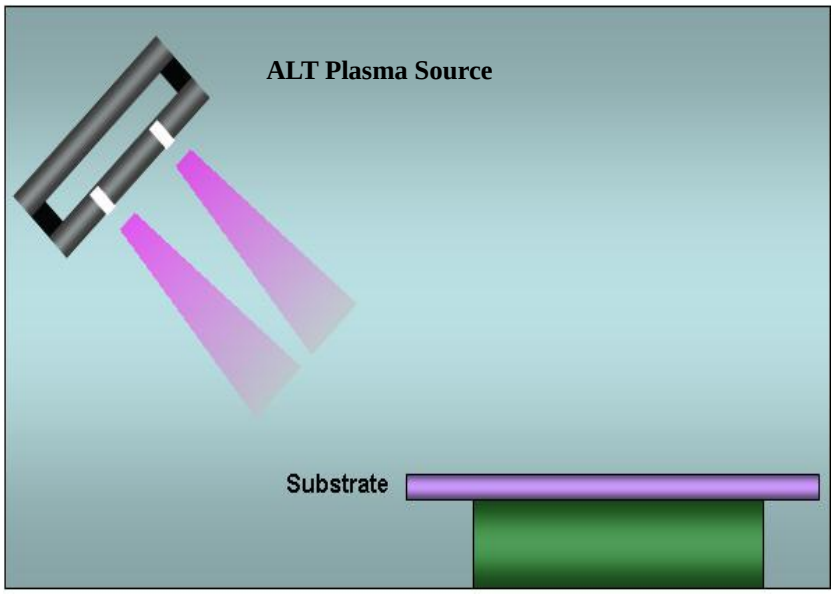

Fig. 2-5 Schematic diagram of ALT plasma system

2.3.2 Application for LC Alignment

The modern LCD is the promising technology of the flat panel display area nowadays. The function of alignment layer inside the cell is to align LC toward desired direction with controllable driving voltages. It should be highly uniform with desirable alignment parameters, such as selective pretilt angle and strong anchoring energy and plays a very important role to influence the electro-optical performance of the LCD. Among many alignment method, rubbing is the widely used process attributed to the simple construction and low cost. However, it is widely recognized and inevitable some existing drawbacks of the rubbing procedure. Debris and

electrostatic discharge are the common disadvantages of the rubbing and have the serious limitation for the development of the LCD, especially for the high resolution and the large size. The development of new alignment process is necessary to vanquish intrinsic problems of rubbing process mentioned above. Among many possible candidates for the alignment methods, particle beam methods are especially attractive.

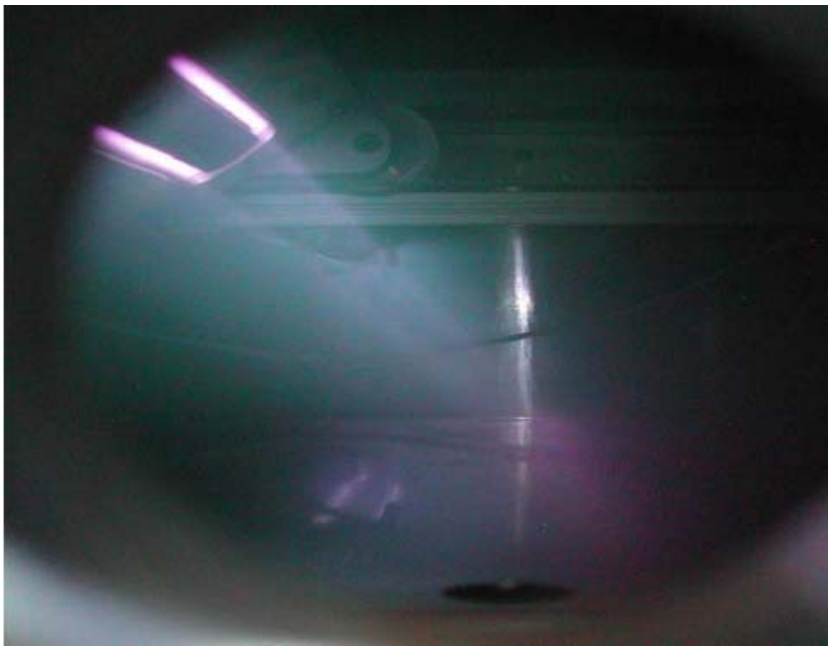

Fig. 2-6 ALT Plasma beam with race-trap sharp

In this experiment, plasma beam alignment technique has been developed for large scale non-contact mode alignment method. The flux of plasma beam obliquely treats on the surface of the alignment substrate and result in the anisotropic property on the alignment surface. Z. M. Sun etl., investigated on the molecular orientation of nematic 5CB on various solid substrates sputtered by an Ar^+ ion beam experimentally in 1994 and is the first research on the LC orientation by this method. [18] Since IBM group studied the organic and inorganic films by atomic beam alignment and

demonstrate the 13.3 inch prototype laptop computer. [19~20] Their idea is based on the treatment with low ion energy and only very top layer of the alignment surface is influenced. Particle beam alignment has been paid great attention to take the place of the conventional rubbing process. Fig. 2-6 shows the ALT plasma beam with race-trap sharp in the chamber. As a result, ALT plasma alignment used in this experiment is the promising technique to substitute for the traditional rubbing method for the next generation.

2.3 Alignment Mechanism

With many disadvantages of associated with mechanical rubbing, non-contact alignment of liquid crystals has the most promising substitution for this conventional method. As a result, plasma alignment was the selection by ALT plasma source in this experiment. Moreover, the alignment mechanism of this non-contact technique had been studied for a long period. Previous studies indicate that bond scission and cross-linking are the major processes on argon ion beam interaction with polymers. Several factors influence the plasma beam bombardment, such as the plasma energy and the chemical structures of the polymers [21~22]. Stohr J. et al. suggested that orientational order is created by preferential bond breaking and bond formation relative to ion beam direction by using near edge X-ray absorption spectroscopy (NEX-AFS) [23]. In addition, X-ray photoelectron spectroscopy (XPS) is usually used simultaneously because NEXAFS does not provide information on the chemical changes produced in the alignment layer during the ion beam bombardment. As a result, polarized attenuated total reflection infrared spectroscopy (ATR-IR) is the better selection because it can provide orientational and chemical information of the polymer surface, which is directly related to the alignment mechanism. J. E. Fulghum

et al. investigated the alignment mechanism of the polyimide (PI 2555) with the instrument, ATR-IR, and suggest that selective destruction of the weakest bonds (π bonds) in the polymer by the argon ion beam result in a net excess of the remaining π bonds, which cause the anisotropy in these π bonds align liquid crystals parallel to the ion beam propagation direction [24].

Chapter 3

Fabrication and Measurement Instruments

3.1 Introduction

New approach adopted ALT plasma alignment technique for OCB mode cells were proposed in this thesis. The fabrication process and measurement instruments will be also described in this chapter.

The fabrication sequences of the proposed method included the substrate, ALT plasma alignment procedure and the cell formulation. The commercial available indium-tin oxide (ITO) glass was cleaned by standard process in advance. Afterwards, the ITO surface was irradiated by UV-Ozone for 30 minutes and then spin coating, a semiconductor process, was utilizing in order to acquire the uniform alignment layer. After the spin coating process, the alignment surface was treated by the ALT plasma source with controllable parameters.

The cell fabrication puts together the ITO substrates with accurate alignment. The cell gap was controlled approximately 5 μm by spacers and the space between the two ITO substrates was filled with the nematic LC (Chisso ZOC-5119xx) for OCB. After cell process, the pretilt angle and electro-optical performance (V-T characteristic, response time, transition voltage) of the OCB cell were investigated.

Moreover, the white and dark states were observed by the polarized optical microscope (POM) and the surface morphology of alignment surface after ALT plasma treatment was investigated by atomic force microscope (AFM). The major features of the instruments mentioned above will be described in detail in this chapter.

3.2 Fabrication Process

3.2.1 Flow chart

The flow chart of the fabrication process of the OCB cells was illustrated as following and provides the overview of the whole cell fabrication process as shown in Fig. 3.1. The ITO glass cleaning, pin coating with polyimide, ALT plasma alignment and cell formulation will be described in detail in the next section.

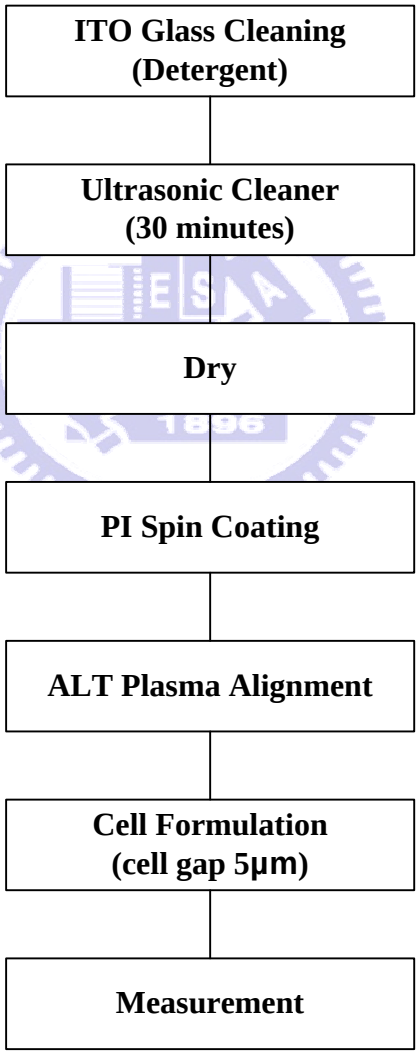

Fig. 3-1 the fabrication flow chart of the OCB cell

3.2.2 Cell Fabrication

(a) Substrate cleaning

The glass was widely used as a substrate for the display application area. As a result, the glass substrate cleaning plays a very important role to influence the display. In the fabrication, the glass of about 1.1 mm thick was selected and ITO was uniformly sputtered on the glass. The ITO glass was firstly cleaned by detergent and then deionized water in an ultrasonic cleaner for 30 minutes and then dried by nitrogen gas. Afterwards, the ITO glass was backed on the hot plate with the temperature, 100°C, for 30 minutes.

(b) Spin coating

After the ITO substrate cleaning, the ITO surface was firstly exposed by the UV-Ozone for 20 minutes. The polyimide (Chisso 5580-01A) was selected and mixed with the solvent (Chisso NBG-667) before spin coating. Right after that, polyimide thin film was spin-coated upon the ITO layer with the lower spin-rate, 800 rpm, for 20 sec and the higher spin-rate, 5000 rpm, for 60 sec. Afterwards, the polyimide thin film was baked on the hot plate at the temperature, 200°C, for 1 hour.

(c) ALT plasma alignment

Throughout the previous two processes, ALT plasma alignment upon the spin-coated polyimide layer is the following step. At the beginning, the inside pressure was pumped to the base pressure, 2×10^{-4} Torr. Afterwards, several

parameters can be controlled during the plasma alignment, such as incidence, gas, exposure time and voltage. In this experiment, investigating the influence of different exposure time toward the alignment surface and electro-optic performance of the OCB cell is our concern. The incidence of the plasma beam source was fixed at 70° and different exposure time (5 sec, 20 sec, 35 sec, 50 sec and 65 sec) was the main parameter. During the plasma alignment process, the gases were introduced into the chamber, such as Ar, H_2 and N_2 with 20 sccm flow rate and the working pressure was 1.25 x 10^{-3} Torr. In addition, the voltage was controlled by 500 V because of the stable plasma environment at this voltage. Table. 3-1 reveals the selected parameters of the ALT plasma alignment and the operation procedure of this alignment is also listed in Table. 3-2.

No.	Time (sec)	Voltage (v)	Ar (sccm)	Incidence (°)
1	5	500	20	70
2	20	500	20	70
3	35	500	20	70
4	50	500	20	70
5	65	500	20	70

Table. 3-1 the parameters of the ALT plasma alignment

Table. 3-2 The procedure of the ALT plasma alignment

Alignment Steps	
1. Incidence	Select the desirable one
2. Bump to Vacuum	Base pressure 2 x 10^{-4} Torr
3. Parameters Setting	Gas flow rates, exposure time
4. Plasma treatment	Working pressure 1.25 x 10^{-3} Torr

(d) Cell formulation

Two crossed ITO Glasses were glued with sealing gel containing spacers. The diameter of spacer with 5 μm is required for maintaining the cell gap. Finally, the space between two substrate was filled with the nematic LC (Chisso ZOC-5119xx).

3.3 Measurement Instruments

After the whole process of the OCB cells, the measurement procedure was started as following, such as pretilt angle, V-T characteristic, transition voltage, response time and surface roughness.

3.3.1 Electro-optical Measurement System

The electro-optical measurement system is shown in Fig. 3-2. This optical system is responsible for the measurement of electro-optical properties, such as V-T characteristics and response time. In the beginning, the intensity of laser source within the acceptable range of the photo detector is needed to be reduced by using a 10% ND

filter. As following, the moderate unpolarized light becomes a polarized light after passing through the polarizer and then enters the LC cell. The LC cell, acted as a phase modulator, changes the phase of the incident polarized light by retardation $\Delta n \cdot d$ (Δn is the birefringence of LC, and d is the thickness of LC). After that, the modulated light passes through the analyzer and the light output is received by the photo detector. The driving waveform of OCB cell is written by ourselves and sent by a waveform generator WFG500 (from FLC Electronics AB). The optical output received by the photo detector can be observed with the oscilloscope (from Tektronix) and quantified data can be read by a multimeter (from Keithley).

We use a bipolar square wave with various frequencies, applying on the cell, to measure the response time of the test cell. The V-T curve is measured by using a 1k Hz bipolar triangular wave.

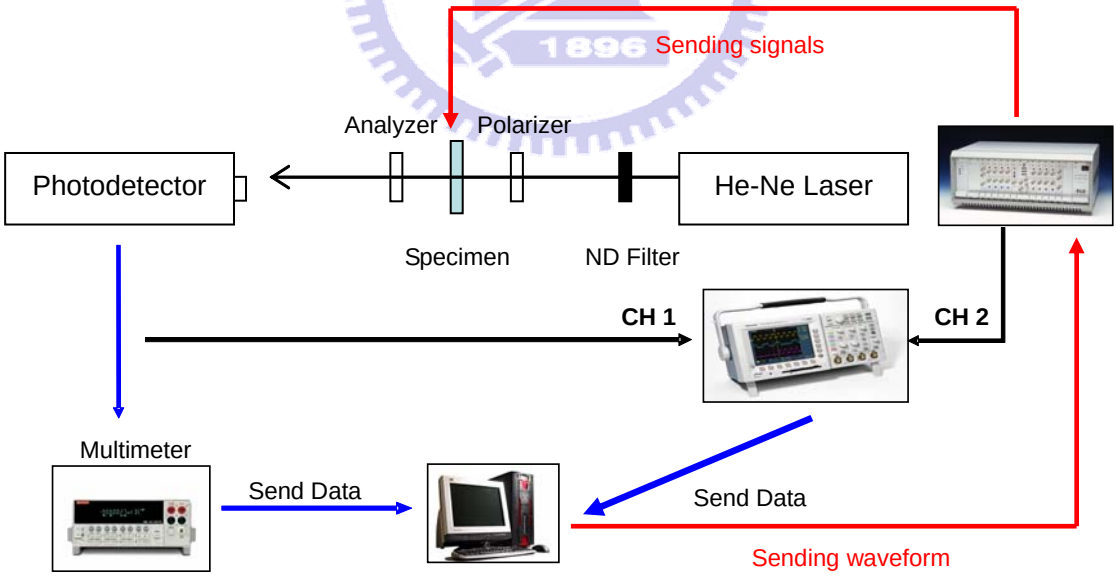

Fig. 3-2 The schematic diagram of electro-optical measurement system

3.3.2 Cell Gap Measurement System

For liquid crystal display, the thickness of cell gap usually affects the optical performance, especially for response time. As a result, the cell gap measurement has to be understood in advance as the following procedure of the measurement. The measurement instrument used is UV/Vis spectrometer LAMBDA 650 from Perkin Elmer, and the principle of this method is introduced as below.

The basic concept of the measurement method is based on the interference of light reflected by the two reflecting surfaces. The illustration is as Fig. 3-3. R1, a coefficient of reflection, is defined as ratio of the light reflected by surface 1 to the incident light. R2 is the reflection coefficient of surface 2.

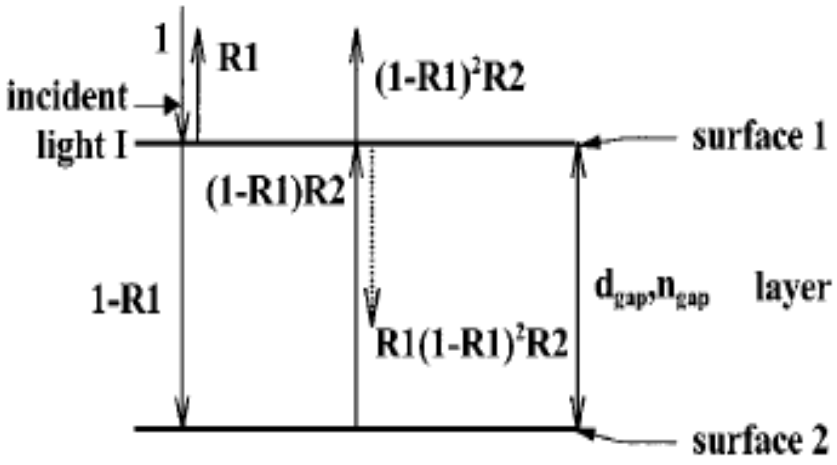

Fig. 3-3 Two reflecting surfaces separated by a layer causing a light interference. The dotted line indicates the first internal reflection

If the total incident light is $I = \cos \omega t$ and there is no any absorption of light in surface 1and 2 was assumed, then we can write the total reflected light R as

$$R = R_1 \cos \omega t + \sum_{k=1}^{\infty} R_1^{k-1} R_2^{k} \left(1 - R_1\right)^{1+k} \cos \omega \left(t - k t_o\right) \qquad (3\text{-}1)$$

Where $\omega = 2\pi c n_{gap}^{\frac{1}{2}} / \lambda$ and $t_0 = 2 d_{gap} n_{gap}^{\frac{1}{2}} / c$, c is the speed of light in the vacuum, λ is the wavelength, d_{gap} is the thickness of the layer, n_{gap} is the refractive index of the layer. The cosine factor in Eq. (3-1) for k>1 are caused by internal reflections. Since R1<1 and R2<1, the magnitude of the cosine factors for k>1 is much smaller than for k=1. Therefore the internal reflection is chosen to be neglected, so

$$R = R_1 \cos \omega t + \left(1 - R_1\right)^2 R_2 \cos\left(\omega t - \frac{4\pi n_{gap} d_{gap}}{\lambda}\right) \qquad (3\text{-}2)$$

Thus the reflected spectrum is

$$\left|R(\lambda)\right|^2 = R_1^{\,2} + \left[\left(1 - R_1\right)^2 R_2\right]^2 + 2R_1\left(1 - R_1\right)^2 R_2 \times \cos\left(4\pi n_{gap} d_{gap} / \lambda\right) \qquad (3\text{-}3)$$

The periodic term in Eq.(3-3) causes an interference pattern. The periodicity of the reflected interference spectrum determined the optical thickness of the cell gap, $n_{gap} d_{gap}$.

If λ_1 and λ_2 are the two wavelengths showing extrema in Eq.(3-3), then $\cos\left(4\pi n_{gap} d_{gap} / \lambda\right) = \pm 1$ for $\lambda = \lambda_1$ and $\lambda = \lambda_2$. Therefore

$$2 n_{gap} d_{gap} = k_1 \lambda_1 / 2 \qquad (3\text{-}4)$$

$$2 n_{gap} d_{gap} = k_2 \lambda_2 / 2 \qquad (3\text{-}5)$$

Where k_1 and k_2 are natural numbers. Suppose $\lambda_1 > \lambda_2$, then

$$k_2 = k_1 + x \tag{3-6}$$

Where x is a natural number.

Based on Eqs.(3-4), (3-5), and (3-6), we can write

$$n_{gap} d_{gap} = \frac{x\lambda_1\lambda_2}{4(\lambda_1 - \lambda_2)} \tag{3-7}$$

The value of x-1 indicates the number of extrema in $|R(\lambda)|^2$ between the wavelengths λ_1 and λ_2. It is better to choose the distance x between the two extrema as large as possible for improving the accuracy of the calculation of $n_{gap} d_{gap}$. The sample data was shown in Fig. 3-4 for a 5.0 μm cell.

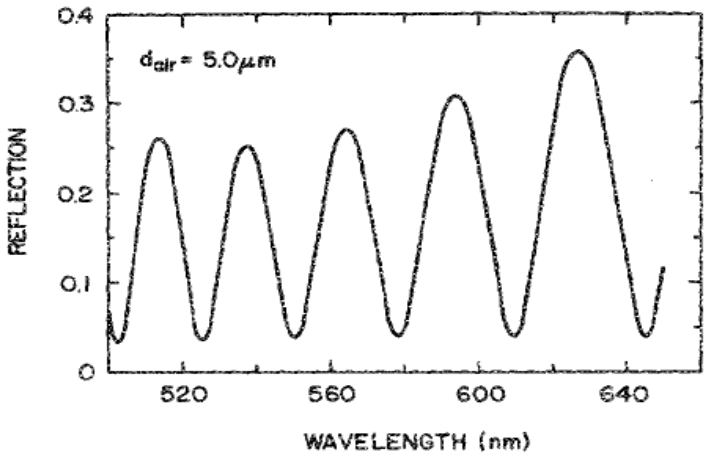

Fig. 3-4 The reflection as a function of wavelength using a air gap of 5.0μm.

3.3.3 Pretilt Angle Measurement System

Fig. 3-5 Pretilt angle measurement system (Autronic DMS 101 TBA)

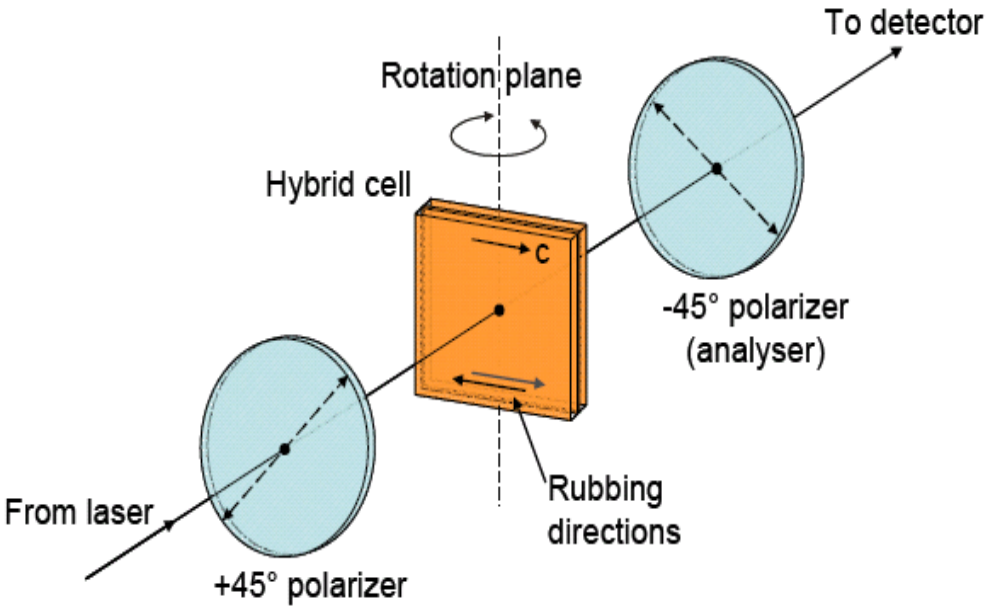

Fig. 3-6 Schematic diagram of crystal rotation method

An anti-parallel symmetric cell was assembled to measure the pretilt angle with the crystal rotation method (Autronic DMS 101 TBA instrument) as shown in Fig. 3-5.

The cell was rotated with rotation stage while the transmitted laser power through the analyzer was measured. The He-Ne laser with the wavelength 632.8mw is the lader source. Stepper driven rotary stage with 2x10-3 degree resolution can measure from planar to homeotropic (0-90 degrees) and cell gap from 20-60um. The schematic diagram of crystal rotation method is shown in Fig. 3-6.

3.3.4 Atomic Force Microscopy (AFM)

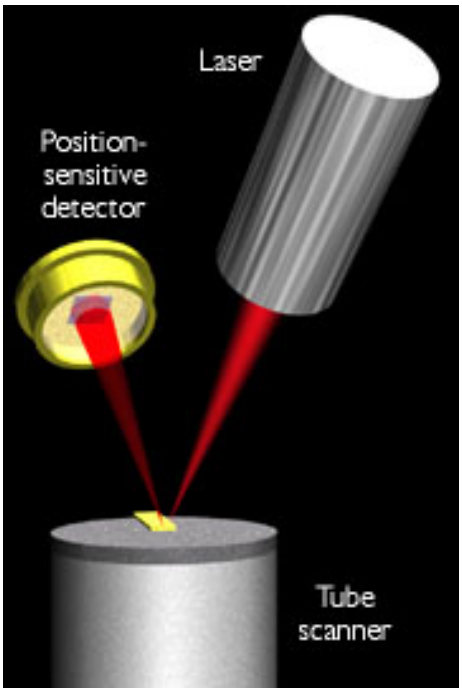

Fig. 3-7 Concept of AFM and the optical lever

AFM consists of a sharp tip mounted on the end of a flexible cantilever spring. Forces from the sample act on the tip and generate some measurable change in the cantilever, such as deflection or shift in resonant frequency. To form an image, the interaction between the sample and tip is mapped to the monitor as a function of position mechanically scanning the sample relative to the tip in a raster pattern into

the photo-detector. By detecting the difference in the photo-detector output voltages, changes in the cantilever deflection or oscillation amplitude are determined. A schematic diagram of this mechanism is depicted in Fig 3-7.

There are two major operation modes for AFM:

(a) Contact mode

Contact mode is the most common method to operate the AFM. As the term suggests, the tip and the sample remain in close contact as the scanning proceeds. One of the drawbacks of remaining in contact with the sample is that there exists a large lateral force on the sample as the tip is dragged on the specimen.

(b) Taping mode

Tapping mode consists of oscillating the cantilever at its resonance frequency (typically hundreds of kilohertz) and positioned above the surface so that it only taps the surface for a very small fraction of its oscillation period. The laser deflection method is used to detect the root-mean-square (RMS) amplitude of cantilever oscillation. The advantage of tapping mode over contact mode is that it eliminates the lateral, shear forces present in contact mode, which enables tapping mode to image soft, fragile, and adhesive surfaces without damaging them.

Chapter 4

Experimental Results and Discussions

4.1 Introduction

The procedure of the OCB cell adopted ALT plasma alignment technique was introduced in previous chapter. As mentioned before, exposure time of the plasma beam is the main factor during the plasma beam alignment. In addition, different plasma exposure time (5 sec, 20 sec, 35 sec, 50 sec and 65 sec) was selected as the main alignment parameter. The electro-optical performance, such as V-T characteristics and response time, of OCB cell will be discussed. Moreover, the pretilt angle dependence and the surface morphology of the alignment layer after plasma beam treatment are measured by TBA and AFM will also be described in detail in this chapter.

4.2 V-T Characteristic

4.2.1 Plasma Alignment Treatment

The transition voltage, which is the voltage from splay state to bend state, is needed as using in the OCB mode as mentioned above. Moreover, V-T characteristics of the OCB cell are a very important analysis, not only the transition voltage but also the white and dark states. Fig. 4-1 shows the V-T characteristics of the OCB cells and compare with plasma and rubbing alignment methods. In this figure, different exposure time (20 sec, 35 sec and 50 sec) are especially discussed with the conventional rubbing method because of its significant alignment parameter in the

plasma treatment.

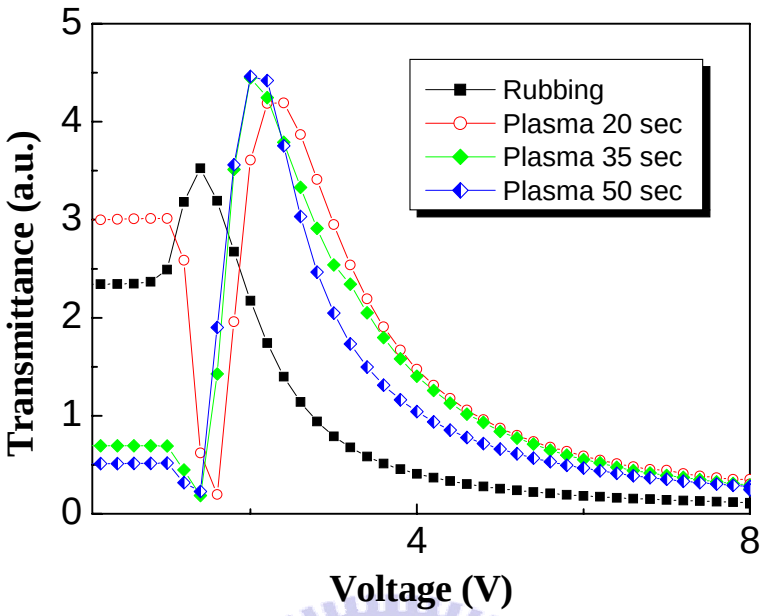

Fig. 4-1 V-T characteristics as different exposure time (20sec, 35sec and 50sec) compare with the rubbing method

The transition voltage by using rubbing process is 1.6v and reveals the lowest one than that of the plasma alignment treatment. Moreover, only concern in the plasma alignment, 20sec and 35sec exposure time provide the lowest transition voltage, 2.2v, than others. Table 4-1 lists the transition voltage of the OCB cells. Furthermore, the white state of rubbing reveals relatively weak transmittance than that of plasma alignment. However, for the dark state phenomena, rubbing method provides the darkest situation and cannot be comparable by plasma alignment treatment. Besides, higher transmittance can be obtained by plasma alignment technique than conventional rubbing method, especially for 50 sec exposure time, which reaches the highest transmittance. As a result, how to improve the disadvantage of relatively weak dark state by plasma alignment is a very important issue.

Table 4-1 List of transition voltage of OCB cells

	Rubbing	Plasma 20sec	Plasma 35sec	Plasma 50sec
Transition Voltage (v)	1.6	2.2	5.0	5.0

4.2.2 Hybrid Cell

As mention in previous section, dark state by plasma alignment cannot be compatible as compare with that by rubbing process. As a result, hybrid cells are fabricated with two kinds of alignment methods and are other solutions to attempt attributed to its dissymmetric cell with two different alignment layers on the two substrates. On the lower polyimide surface conventional rubbing is used and in the contrast on the upper one plasma alignment treatment is the selected procedure.

Rubbing is the alignment method adopted in this research, which is generally carried out by moving the substrate with a constant velocity under a rotating roller covered with a velvet cloth. The rubbing force are varied with the rubbing process parameters such as the roller diameter and the rotation speed, the substrate advancing speed, number of rubbings, and the pile impression (the depth of the rubbing cloth pressed down by roller). The rubbing strength (RS) defined by Seo *et al.* [] is as following

$$RS = NM\left(2\pi rn / V - 1\right)$$

Where N is the number of rubbings (N=1 in our experiments), M is the depth of the deformed fibers of the cloth, n is the rotation speed of the roller (300/60 s^{-1}), V is the

advancing speed of the substrate (7.3 mm/s), and r is the radius of the roller (22.5 mm). The RS is given in mm unit.

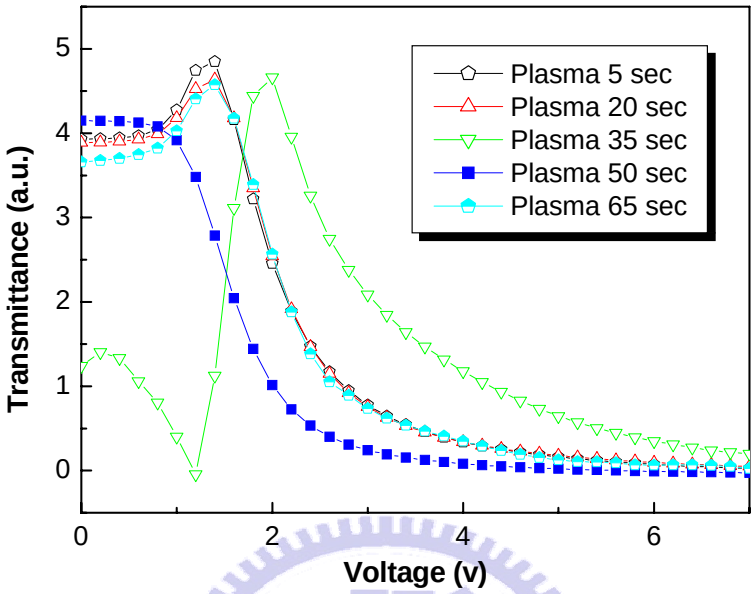

Fig. 4-2 V-T characteristics as different exposure time (5sec, 20sec, 35sec, 50sec and 50sec) with hybrid OCB cells

The transmittance dependence with hybrid cell as function of plasma exposure time is shown in Fig. 4-2. The white state under plasma exposure time (5sec, 20sec, 35sec and 65sec) indicates the stable transmittance. However, the worst transition voltage, 2v, is revealed with 65sec plasma exposure time. Besides, the dark state are all improved as compare with the hybrid cells and pure plasma ones. Fig. 4-3 shows the comparison of dark state between the pure plasma alignment cell (50sec) and hybrid cell (rubbing and plasma 50sec). Furthermore, the dark state can be apparently improved by using hybrid cell compared with the pure plasma alignment cell. Table 4-2 lists the transition voltage of the hybrid cells.

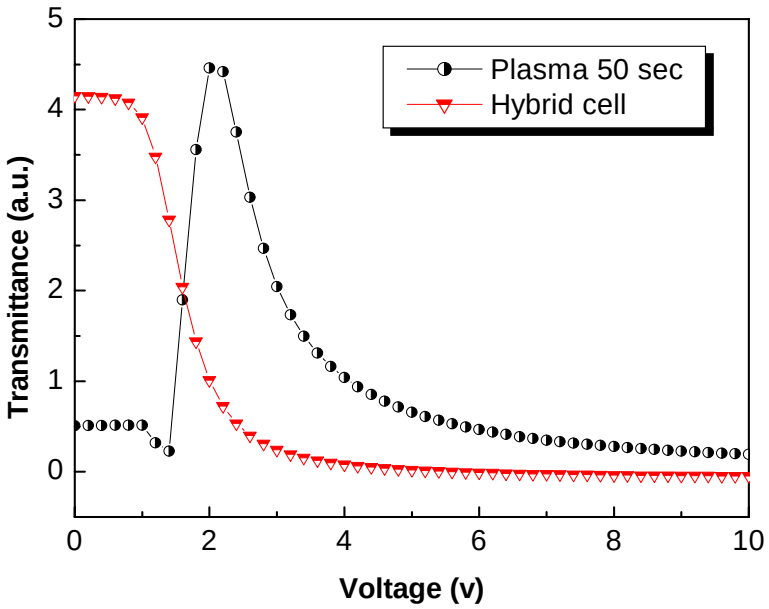

Fig. 4-3 V-T characteristics as 50sec plasma exposure time compare with hybrid cell

Table 4-2 List of transition voltage of hybrid cells

	Rubbing	Plasma 20s	Plasma 35s	Plasma 50s	Plasma 65s
Transition Voltage(v)	1.4	1.4	2.0	0	1.4

4.3 AFM Analysis

The destruction of the weakest bonds in the polymer was revealed during the plasma alignment as mentioned in previous study. Besides, surface morphology of the surface of the polyimide is also an important factor, since the LC molecule directly attaches the surface. The thickness dependence of the polyimide as function of plasma exposure time is shown in Fig. 4-4. The original thickness of polyimide before plasma treatment is 60nm. However, after plasma bombardment, the thickness decreases

linearly as the increase of the exposure time. Eventually, the thickness remains 42nm even though after 65sec plasma treatment. According to this result, thickness of polyimide decrease as the plasma exposure time increase is revealed. Furthermore, the surface morphology of the polyimide surface before and after plasma treatment is indicated in Fig. 4-5 (a), (b) and (c). The original surface of polyimide before plasma alignment is shown in Fig. 4-5 (a). Then, Fig. 4-5 (b) and Fig. 4-5 (c) indicate the surface morphology after 20sec and 65sec plasma treatment. The 3D surface morphology of these surfaces are also shown in Fig. (d) and Fig. (e). It indicates that the surface morphology changed as the increase of exposure time and seen to become rougher on the surface after plasma bombardment visually.

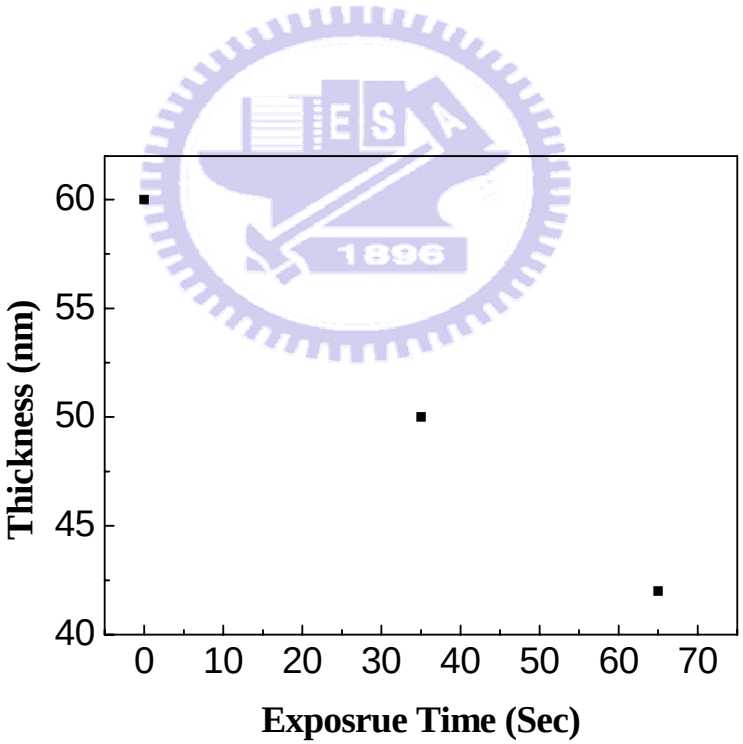

Fig. 4-4 Dependence of thickness of polyimide as function of exposure time

Beside the surface morphology of polyimide, the surface roughness is also investigated simultaneously as shown in Fig. 4-6. The surface roughness without any

plasma treatment shows the lowest one, 0.23nm, than that with plasma alignment. Dependence of surface roughness after plasma beam bombardment increase gradually until 50sec. The maximum surface roughness, 0.48nm, is revealed at 50sec plasma treatment. Eventually, the surface roughness decrease to 0.43nm after 65sec and controllable surface roughness can be indicated after 35sec plasma alignment. According to these result, surface roughness of polyimide are changed apparently after the plasma treatment especially for the increase of exposure time and indicate that is the main factor during this process.

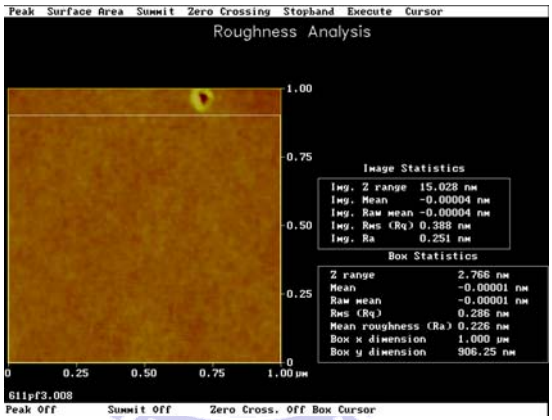

(a)

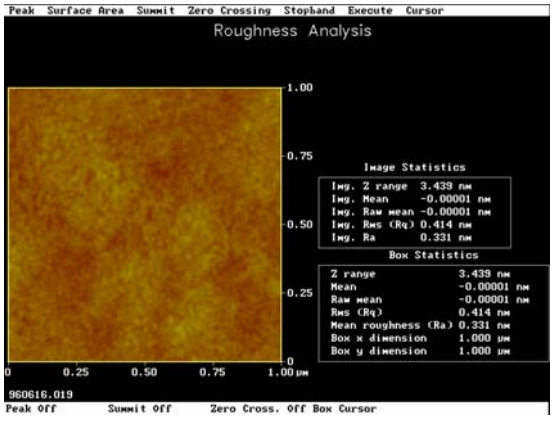

(b)

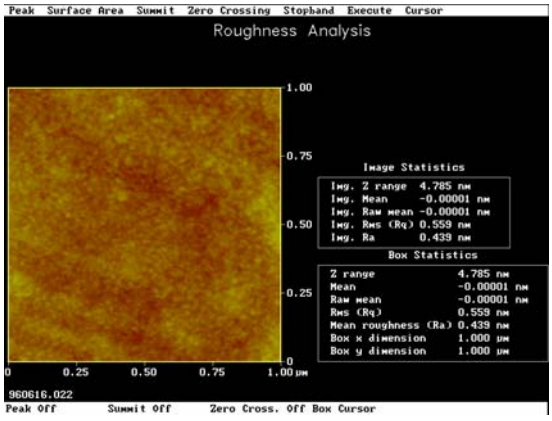

(c)

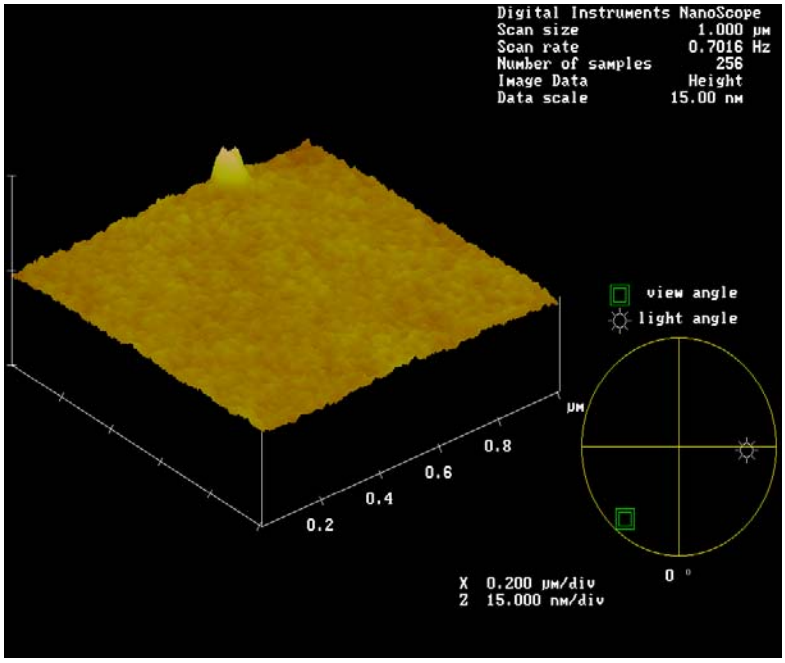
Digital Instruments NanoScope
Scan size 1.000 µm
Scan rate 0.7016 Hz
Number of samples 256
Image Data Height
Data scale 15.00 nm
view angle
light angle
µm
0.2
0.4
0.6
0.8
0 °
X 0.200 µm/div
Z 15.000 nm/div

(d)

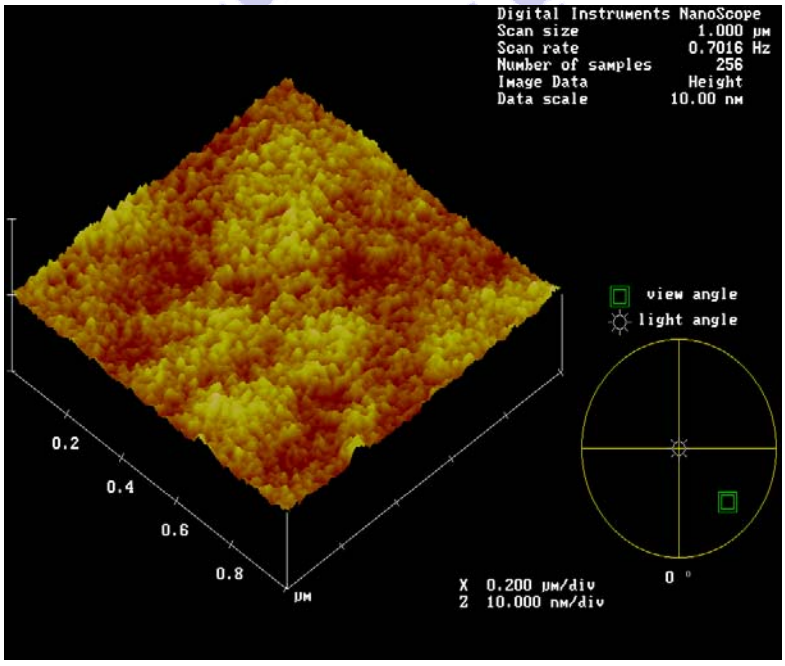
Digital Instruments NanoScope
Scan size 1.000 µm
Scan rate 0.7016 Hz
Number of samples 256
Image Data Height
Data scale 10.00 nm
view angle
light angle
0.2
0.4
0.6
0.8
µm
0 °
X 0.200 µm/div
Z 10.000 nm/div

(e)

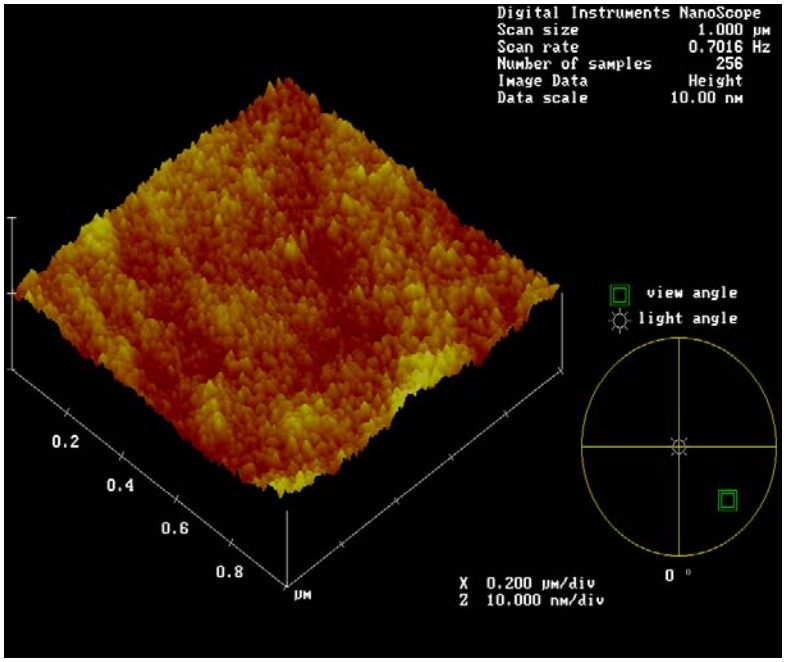

(f)

Fig. 4-5 Surface morphology of polyimide (a) original surface

(b) 20sec plasma treatment (c) 65sec plasma treatment

(d) 3D before plasma (e) 3D after plasma 20sec

(f) 3D after plasma 65sec

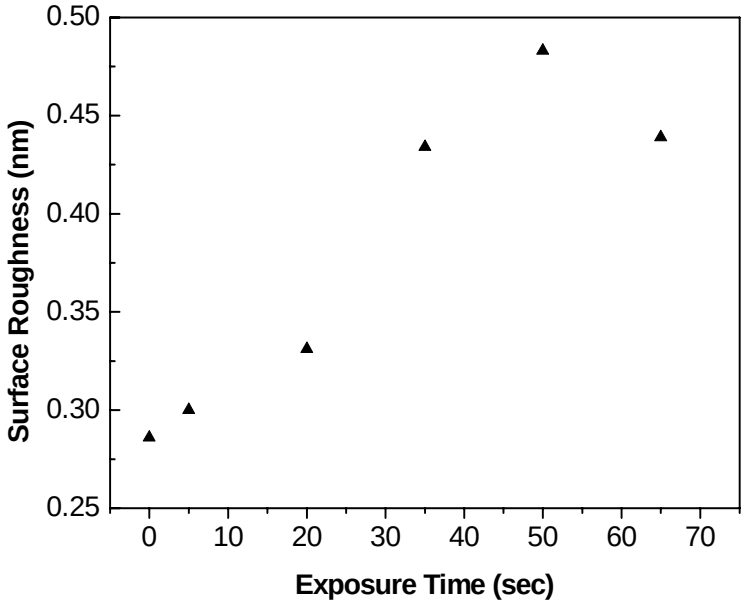

Fig. 4-6 Surface roughness as function of exposure time

4.4 Pretilt Angle Dependence

The operation of liquid crystal display requires monodomain alignment and control of pretilt angle of LC molecules on the substrate surface. The pretilt angle prevents the creation of reverse tilted disclinations in twisted nematic LCD. Furthermore, pretilt angle plays a very important role and also influence the LC alignment stability and electro-optical (EO) characteristics of LC operation modes using polyimide thin films. Fig. 4-7 shows the pretilt angle dependence as function of plasma exposure time (5sec, 20sec, 35sec, 50sec and 65sec). The 1.8° pretilt angle appeared only after 5 sec plasma beam treatment. Dependence is non-monotonous going through maximum. The pretilt angle increases gradually after 5 sec and maximum pretilt angle is revealed at 65 sec. However, in the case of original polyimide thin films, the pretilt angle does not exist. It believes that plasma beam exposure time is the main factor in generating a LC pretilt angle.

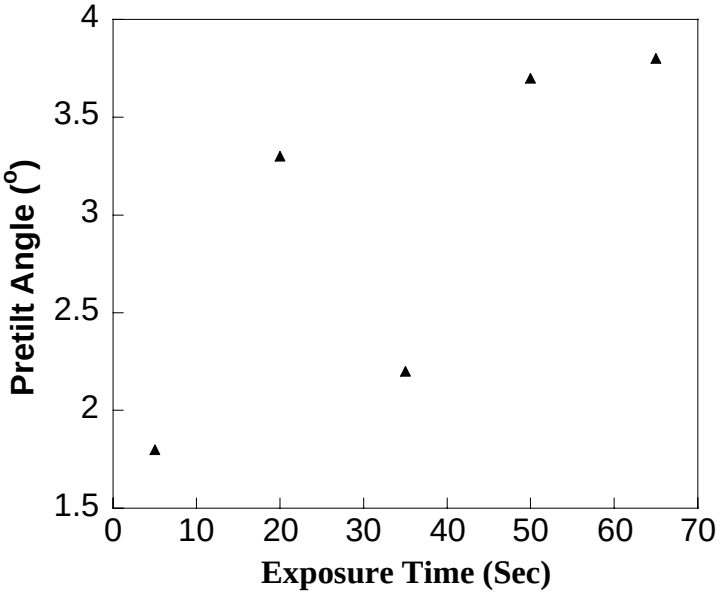

Fig. 4-7 Pretilt angle dependence as function of exposure time

O.V. Yaroshchuk et al. suggest that selective destruction of the weakest bonds (π bonds) in the polymer by the argon ion beam result in a net excess of the remaining π bonds, which cause the anisotropy in these π bonds align liquid crystals parallel to the ion beam propagation direction [24]. As mention in Fig. 4-6, the surface roughness increase as function of plasma exposure time. Compare with the Fig. 4-6 and Fig 4-7, it seens that the dependence between pretilt angle and surface roughness is not apparent during this period of exposure time. In addition, the influence of the surface energy to pretilt angle is the possible factor. It is because that the surface energy of the polyimide shows the relative dependence with the destruction of the weakest bonds in the polymer. As the exposure time increase, the more destruction of the weakest bonds is obtained and causes the decrease of surface energy. In addition, the interaction between LC and alignment films becomes weak which results in the increase of pretilt angle as function of plasma exposure time.

4.5 POM Characteristics

Alignment property which can be investigated by POM is also an important factor, especially for OCB mode because the transition from splay to bend state is necessary. The dark and white state of the OCB cell as function of plasma exposure time can be investigated according to the POM. Fig. 4-8 shows the dark state of OCB cells as function of plasma treatment with the driving voltage, 10v. As shown in Fig. 4-8 (a) and 4-8 (b) it remains some defect area and indicates that the totally transition from splay to bend can not be occurred after 5sec and 20sec plasma alignment. Compare with Fig. 4-8 (c) and 4-8 (d), the better dark state can be revealed at 50sec plasma alignment. Moreover, the V-T characteristic of hybrid cell provides the

excellent dark state than that of pure plasma alignment mentioned previously. The dark states of hybrid cells are also investigated by POM as shown in Fig. 4-8 (e). According to this analysis, hybrid cell provides the very dark state than any others visually.

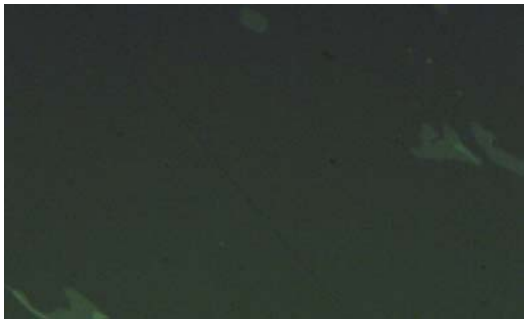

(a) plasma 5sec

(b) plasma 20sec

(c) plasma 50sec

(d) plasma 65sec

(e) hybrid cell

Fig. 4-8 Dark state for OCB cell as function of plasma exposure time after driving 10v

4.6 Response Time

Response time is another important factor for LCD TV. TV images generally consist of moving pictures, and most LCDs have slow response time compared to other display devices. Especially for the motion blur problem attributed to the slow response time is a critical factor is needed to improve. As a result, OCB mode is a possible candidate to improve such important issue because of its relatively fast response time.

The response time of OCB cell which made by ALT plasma alignment technique was investigated. Cell gap of each OCB cells are kept in 5 μm to maintain the precision of the response time. The dependence of response time of OCB cell as function of plasma exposure time is shown in Fig. 4-9. The fastest and slowest response time of OCB cell is revealed between 3.3ms and 4ms according to the experiment. Furthermore, it shows non-dependence of the response time and different exposure time of OCB cells. In addition, it has to be paid attention on the 50sec plasma exposure time because of its relatively fastest response time. The fastest response time, 3.3ms, adopted by plasma alignment shows the compatible potential to challenge that by conventional rubbing process. Fig. 4-10 indicates the comparison of the response time and pretilt angle as function of exposure time. The data shown here also indicated an inverse proportion of pretilt angle and response time with plasma exposure time. As a result, higher pretilt angle related to the fast response time can be obtained in this experiment. Besides, the surface of polyimide after plasma bombardment seems to indicate the relatively influence toward the response time of the OCB cell. It is because that various surface morphology is arisen from the different plasma exposure time. In conclusion, that is the reason why exposure time plays a very important role in the plasma alignment technique.

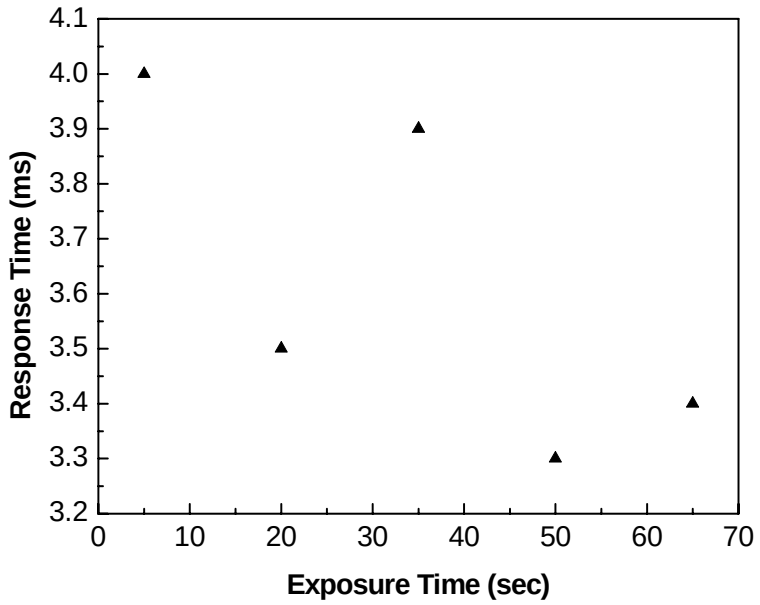

Fig. 4-9 Response time dependence as function of plasma exposure time

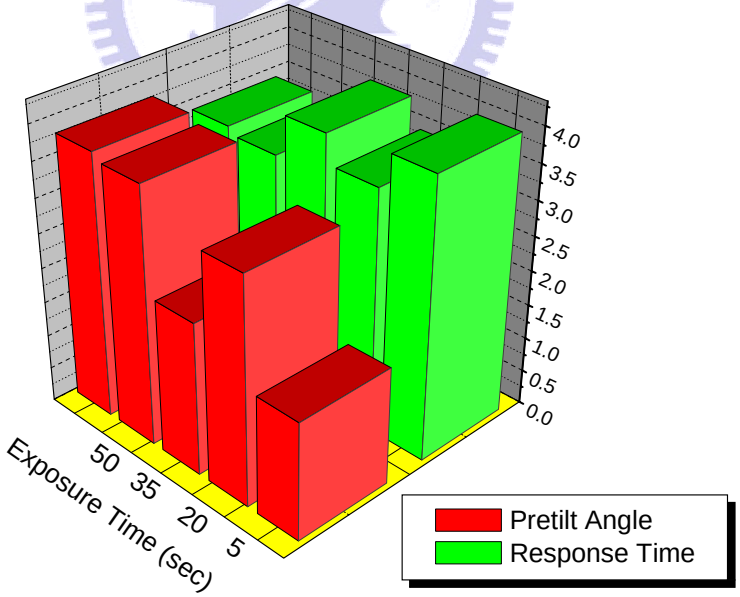

Fig. 4-10 Comparison between pure plasma and hybrid cells

Chapter 5

Conclusions

5.1 Conclusions

ALT (Anode Layer thruster), originally was used for the satellite propulsion in Russia, was modified to be the plasma source for the application of LC alignment technique The ALT source consists of outer and inner cathode and anode. Permanent magnet is necessary to generate magnet pole at outer cathode. The plasma flux is generated by cross electric field (E) and magnetic field (H) immediately. In contrast to current rubbing manufacturing process, the plasma alignment has fewer problems of electrostatic charge and debris and is the potential candidate to replace conventional rubbing process for the next generation large display. The OCB (Optically Compensated Bend) mode LC is known for its fast response time and wide viewing angle. However, rubbing is still the main alignment method for OCB. In addition, the electro-optical characteristics, pretilt angle of OCB cells and surface morphology of alignment layer after plasma treatment were investigated. The influence of OCB cells between these two alignments was also be discussed.

For the V-T characteristics, higher transmittance can be obtained by plasma alignment technique than conventional rubbing method, especially for 50 sec exposure time, which reaches the highest transmittance. However, for the dark state phenomena, rubbing method provides the darkest situation and cannot be comparable by plasma alignment treatment. As a result, hybrid cell is a solution to improve this disadvantage. According to the V-T analysis and POM, the dark state can be apparently improved by using hybrid cell compared with the pure plasma alignment

cell. In AFM analysis, thickness of polyimide decrease as the plasma exposure time increase is revealed. Furthermore, surface roughness of polyimide are changed apparently after the plasma treatment especially for the increase of exposure time and the roughest one is revealed after 50sec plasma treatment. For the pretilt angle dependence, it increases gradually after 5 sec and maximum pretilt angle is revealed at 65 sec. Besides, as the exposure time increase, the more destruction of the weakest bonds is obtained and causes the decrease of surface energy. In addition, the interaction between LC and alignment films becomes weak which results in the increase of pretilt angle as function of plasma exposure time. For the response time characteristics, the fastest response time, 3.3ms, was obtained after 50sec plasma treatment. However, the response time of hybrid cell cannot provide enough fast response time, even though it has well dark state. Besides, the surface of polyimide after plasma bombardment seems to indicate the relatively influence toward the response time of the OCB cell. It is because that various surface morphology is arisen from the different plasma exposure time. In conclusion, that is the reason why exposure time plays a very important role in the plasma alignment technique.

5.2 Future Work

Pure argon plasma alignment was firstly used for OCB cells in this study. The electro-optical (EO) properties, pretilt angle and surface morphology were already investigated. Moreover, the characteristics of anchoring energy after plasma alignment are also another critical issue because anchoring energy is relative to the image sticking problem. Furthermore, the alignment mechanism of plasma treatment is also important factor that need to be studied. The relationship between E-O properties and the alignment mechanism can be discussed.

Reference

[1] M. Katayama, *Japan Display '89. Proc. 9th IDRC*, p.6 (1989)

[2] T. Uchida, T. Nakayama, T. Miyashita, T. Ishinaba, *Asia Display' 95, Proc. 15th IDRC*, p. 599 (1995)

[3] M. Kubo, Y. Narutaki, S. Fujioka, Y. Maruyama, T. Shimada, Y. Yoshimura, M. Katayama, Y. Ishii, S. Yamakawa, A. Ban, U.S. patent 6295109 B1 (2001)

[4] D. K. Yang, J. W. Doane, SID Intl. *Symp. Digest Tech. Papers*, 23, 759 (1992)

[5] P. J. Bos and K. Koehler-Beran, *Mol. Cryst. Liq. Cryst*, 133, 329 (1984)

[6] C. T. Kuo, T. Miyashita, M. Suzuki and T. Uchida, *SID'94 Digest*, p. 927 (1994)

[7] H. Mori and P. J. Bos, *Jpn. J. Appl. Phys*, vol. 38, p. 2837 (1999)

[8] H. Mori, Y. itoh, Y. Nishiura, T. Nakamura and Y. Shinagawa, *SID'97 Digest*, p. 941 (1997)

[9] H. Mori and P. J. Bos, *SID'98 Digest*, LP-J (1998)

[10] Y. Ito, R. Matsubara, R. Nakamura, M. Nagai, S. Nakamura, H. Mori, and K. Mihayashi, *SID'05 Digest*, p. 986 (2005)

[11] J. S. Gwag, J. C. Kim and T. H. Yoon, *Jpn. J. Appl. Phys*, vol. 45, No. 9A, p. 7047 (2006)

[12] N. Koma, T. Miyashita, T. Uchida, and N. Mitani, *SID'00 Digest*, p. 632 (2000)

[13] W. Gibbons, P. Shannon, S. Sun and B. Swetlin, *Nature*, 351, 49 (1991)

[14] M. Hasegawa and Y. Taira, *Proc. 14th IDRC*, p.213 (1994)

[15] Y. Kawanishi, T. Takimiya and K. Ichimura, *Polym. Mater. Sci. Eng*, 66, 263 (1992)

[16] T. Yoshida, T. Tanaka, J. Ogura, H. Wakai and H. Aoki, *SID'97 Digest*, p. 841

(1997)

[17] G. James and R. S. Lowder, *Phys. Fluid,*vol. 9, 1115 (1966)

[18] Z. M. Sun, J. M. Engels, I. Dozov and G. Durand, *J. Phys. II France*, vol. 4, 59 (1994)

[19] P. Chaudhari, J. A. Lacey, S. C. A. Line and J. L. Speidell, *Jpn. J. Appl. Phys.* vol. 37, p. L55 (1998)

[20] P. Chaudhari et al., *Nature*, vol. 411, 3-May (2001)

[21] Share, K., Eichhorn, K. J., Simon, F., Pleul, D., Janke, A., & Gerlach, G. *Surface and Coating Technology*, 139, p. 257 (2001)

[22] Dong, H. & Bell, T., *Surface and Coating Technology*, 111, p. 29 (1999)

[23] Stohr, J., Samant, M. G., Luning, J., et al., *J. Science*, 292, p. 2299 (2001)

[24] J. E. Fulghum, L. Su, K. Artyushkova, J. L. West and Y. Reznikov, *Mol. Cryst. Liq. Cryst*., vol. 412, p. 361 (2004)